Original Article

Clinical significance and immune landscape of cuproptosis-related lncRNAs in kidney renal clear cell carcinoma: a bioinformatical analysis

Ding Li[1,2,3#^], Xuan Wu[4#], Wenping Song[1,2,3], Cheng Cheng[4], Lidan Hao[4], Wenzhou Zhang[1,2,3]

[1]Department of Pharmacy, The Affiliated Cancer Hospital of Zhengzhou University and Henan Cancer Hospital, Zhengzhou, China; [2]Henan Engineering Research Center for Tumor Precision Medicine and Comprehensive Evaluation, Henan Cancer Hospital, Zhengzhou, China; [3]Henan Provincial Key Laboratory of Anticancer Drug Research, Henan Cancer Hospital, Zhengzhou, China; [4]Department of Internal Medicine, The Affiliated Cancer Hospital of Zhengzhou University and Henan Cancer Hospital, Zhengzhou, China

Contributions: (I) Conception and design: D Li, X Wu, W Zhang; (II) Administrative support: W Zhang; (III) Provision of study materials or patients: D Li, X Wu; (IV) Collection and assembly of data: D Li, W Song, C Cheng, L Hao; (V) Data analysis and interpretation: D Li, X Wu; (VI) Manuscript writing: All authors; (VII) Final approval of manuscript: All authors.

[#]These authors contributed equally to this work.

Correspondence to: Wenzhou Zhang. Department of Pharmacy, The Affiliated Cancer Hospital of Zhengzhou University and Henan Cancer Hospital, Zhengzhou 450008, China. Email: hnzzzwzx@sina.com.

Background: Kidney renal clear cell carcinoma (KIRC) is considered an immunogenic tumor. Cuproptosis is a newly identified copper-induced regulated cell death that relies on mitochondria respiration. Long noncoding RNAs (lncRNAs) have emerged as significant players in tumorigenesis and metastasis. However, there is a huge knowledge gap on the prognostic role of cuproptosis-related lncRNAs in KIRC. And, the clinical value of them is still unknown. Here, we aimed to develop a cuproptosis-related lncRNA prognostic signature in KIRC.

Methods: The messenger RNA (mRNA)/lncRNA expression profiles and the clinical information including age, gender, tumor stage, grade, and overall survival (OS) were acquired from The Cancer Genome Atlas (TCGA) database. The included KIRC samples were further randomly assigned into training (n=258) or testing (n=257) data sets. We performed Pearson correlation analysis to identify the cuproptosis-related lncRNAs and then constructed the prognostic signature using Cox regression analysis and LASSO algorithm. Subsequently, Kaplan-Meier survival analysis, a nomogram, and receiver operating characteristic (ROC) curve were performed to assess the predictive performance of the signature. Moreover, the immune characteristics and drug sensitivity related to the signature were also explored.

Results: The signature comprised 7 cuproptosis-related lncRNAs. The patients with a low-risk score had superior OS compared with those with a high-risk score. The survival rates of the high- and low-risk groups were 44.96% and 83.72% (P<0.001). The area under the curve (AUC) value for 1-, 3-, 5-year survival rate reached 0.814, 0.762 and 0.825, respectively. In addition, a nomogram was also generated; the AUC was 0.785 for risk score, higher than that for age (0.593), gender (0.489), grade (0.679), and stage (0.721). The high-risk group had more enriched immune- and tumor-related genes. Patients with low-risk scores were more sensitive to immunotherapy and the small molecular drugs GSK1904529A, tipifarnib, BX-912, FR-180204, and GSK1070916. Meanwhile, the high-risk group tended to be more sensitive to pyrimethamine, MS-275, and CGP-60474.

Conclusions: Collectively, we constructed a cuproptosis-related lncRNA prognostic signature with a higher predictive accuracy compared to multiple clinicopathological parameters, which may provide vital guidance for therapeutic strategies in KIRC. Combination of more prognostic biomarkers may further improve the accuracy.

^ ORCID: 0000-0002-0967-7021.

Keywords: Cuproptosis; lncRNA; prognosis; drug sensitivity; kidney renal clear cell carcinoma

Submitted Oct 10, 2022. Accepted for publication Nov 15, 2022.
doi: 10.21037/atm-22-5204
View this article at: https://dx.doi.org/10.21037/atm-22-5204

Introduction

Renal cell carcinoma (RCC) is a common deadly disease which comprises a number of subtypes characterized by different genetic drivers (1). Kidney renal clear cell carcinoma (KIRC) remains the most prevalent histological type of RCC and accounts for more than 70% of cases (2,3).

Over the past decade, insights in the determinants of KIRC ontogeny and heterogeneity as well as lethality have led to the development of robust mechanistic pathways that recapitulate tumor ontogeny and progression, and are creating subcategories of KIRC patients that may benefit from subtype-specific therapeutic interventions (4). The lack of sensitivity to chemotherapy and radiation therapy prompted research efforts into novel treatment options. Although KIRC is characterized by the genetic mutations-induced hypoxia signaling pathway, which results in heightened angiogenesis, metabolic dysregulation, deleterious tumor microenvironmental (TME) crosstalk, and intra-tumoral heterogeneity, the specific genetic variances identified have contributed to therapeutic innovation and improved the prognosis of KIRC patients (5). The treatment of KIRC has transitioned from a non-specific immune approach, to targeted therapy, and now to novel therapeutic agents, especially immune-checkpoint inhibitors (ICIs), based on significant activity in patients with advanced KIRC (6). Despite these advances, the potential biomarkers for treatment efficacy, candidate patients, and the sequencing and optimal combination of agents remain unavailable (7). Therefore, new early diagnostic biomarkers and treatment targets are still needed to improve the prognosis of cancer patients.

Traditionally, the prognostic prediction in KIRC patients based on the pathologic and clinical factors, including tumor-node-metastasis (TNM) stage, grade, Eastern Cooperative Oncology Group (ECOG) performance status, and absence or presence of necrosis (1). Due to tumor heterogeneity, however, the survival status of patients will be various even in the same stage. The bioinformatic analysis of RNA-sequencing and clinical data have provided novel insights for the mechanistic studies in tumorigenesis and development. Although many prognostic signatures have been developed based on different hallmarks of cancer in KIRC, the limitations involved in them hinder the further application in clinical practice. To explore the more favorable signature for use in clinical practice, novel signatures associated with the new hallmark of cancers required further study.

Previous studies have shown that unbalanced copper (Cu) homeostasis contributed to tumor growth, resulting in irreversible damage (8,9). Cu can cause multiple types of cell death, including autophagy and apoptosis based on different mechanisms, including proteasome inhibition, reactive oxygen species accumulation, and anti-angiogenesis. Hence, Cu ionophores have shown promising potential in the field of tumor treatment and have attracted tremendous attention. Long noncoding RNAs (lncRNAs) have been characterized by their multiple regulatory roles throughout tumorigenesis and metastasis over the past decade. Targeted therapy against lncRNAs is an attractive strategy for the treatment of many diseases, including

Highlight box

Key findings

- We constructed a cuproptosis-related long noncoding RNAs (lncRNAs) prognostic signature with a higher predictive accuracy compared to multiple clinicopathological parameters, which may provide vital guidance for therapeutic strategies in kidney renal clear cell carcinoma (KIRC).

What is known and what is new?

- Cuproptosis is a newly identified copper-induced regulated cell death that relies on mitochondria respiration. LncRNAs have emerged as significant players in tumorigenesis and metastasis. However, the clinical value of cuproptosis-related lncRNAs in KIRC is still unknown. Here, we developed a novel cuproptosis-related lncRNA prognostic signature in KIRC.

What is the implication, and what should change now?

- We identified the important role of cuproptosis-related lncRNAs in KIRC and constructed a prognostic signature, which might serve as a promising biomarker for predicting the prognosis of KIRC patients. While, these findings were mainly based on the integrated bioinformatical analysis, further experimental verification is needed.

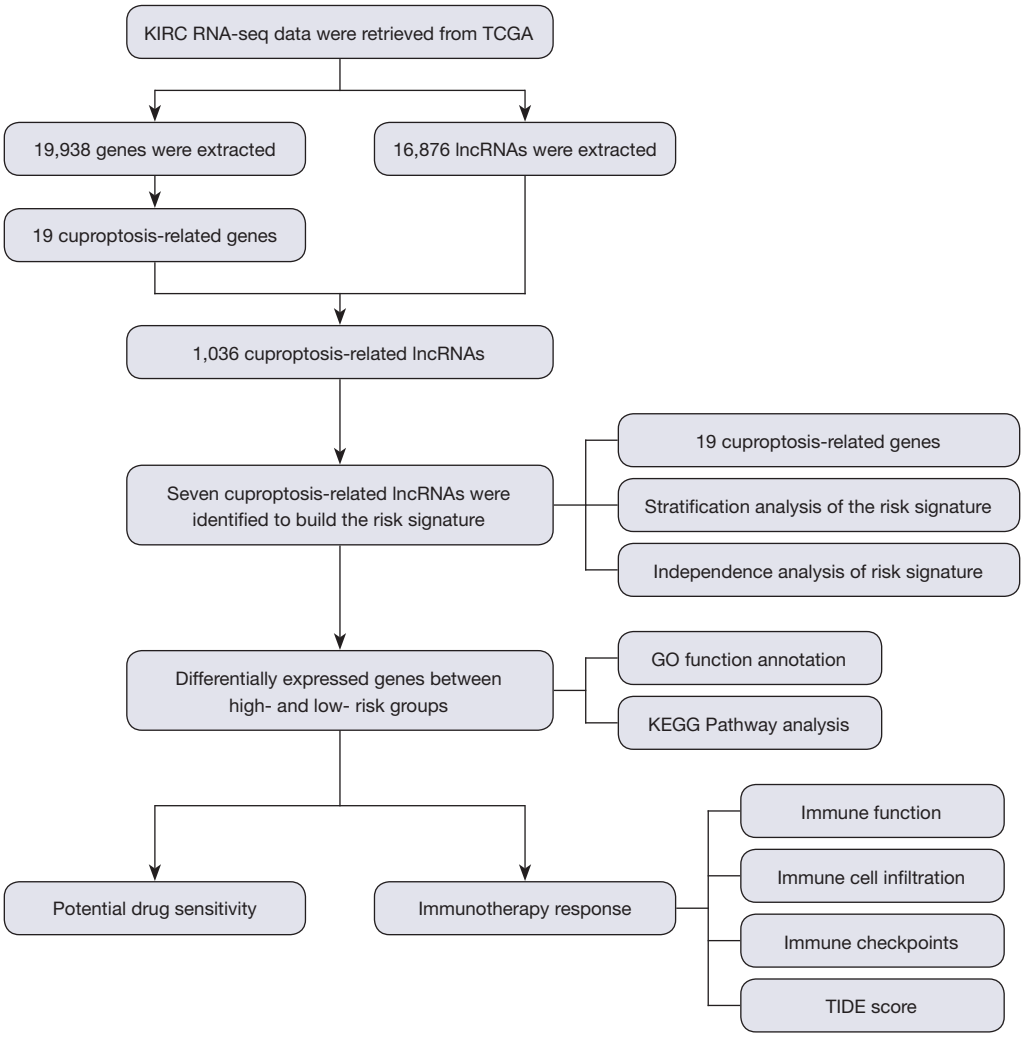

Figure 1 The flowchart of this study. KIRC, kidney renal clear cell carcinoma; TCGA, The Cancer Genome Atlas; GO, Gene Ontology; KEGG, Kyoto Encyclopedia of Genes and Genomes; TIDE, tumor immune dysfunction and exclusion.

cancers (10). Substantial efforts have been made towards the clinical application of RNA-target therapeutics, mainly including antisense oligonucleotides and small interfering RNAs, some of which have been approved by the US Food and Drug Administration (FDA). However, there is a huge knowledge gap on the prognostic role of cuproptosis-related lncRNAs in KIRC. And, the clinical value of them is still unknown.

In the study, we comprehensively analyzed cuproptosis-related lncRNAs in the prognostic and immune landscape of KIRC and conducted a risk prognostic signature, which has a higher predictive accuracy than traditional clinical variables, and provide a view to promote the understanding of KIRC biology and develop promising emerging therapeutic approaches. We present the following article in accordance with the TRIPOD reporting checklist (available at https://atm.amegroups.com/article/view/10.21037/atm-22-5204/rc).

Methods

Clinical specimens and study design

The flowchart of this study design is shown in *Figure 1*. The RNA sequencing profiles, as well as the relevant clinical features, including age, American Joint Committee on Cancer (AJCC) stage, TNM stage, grade, gender, and survival status, of 537 KIRC patients and 72 normal controls were retrieved from The Cancer Genome Atlas (TCGA)

database on 2 June 2022. In total, 515 patients with RNA sequencing profiles and overall survival (OS) were included in this study. Subsequently, the RNA-sequencing data were measured and preprocessed using the method previously described (11). A total of 16,876 lncRNAs were identified. The mRNA expression profiles of 19 cuproptosis-related genes (*SLC31A1*, *PDHA1*, *PDHB*, *NLRP3*, *NFE2L2*, *MTF1*, *LIPT2*, *LIPT1*, *LIAS*, *GLS*, *GCSH*, *FDX1*, *DLST*, *DLD*, *DLAT*, *DBT*, *CDKN2A*, *ATP7B*, and *ATP7A*) were obtained from the previous study. The correlation between these lncRNAs and 19 cuproptosis-related genes was evaluated through Pearson correlation analysis, and 1,036 cuproptosis-related lncRNAs were subsequently identified. The study was conducted in accordance with the Declaration of Helsinki (as revised in 2013).

Construction and validation of the cuproptosis-related lncRNA prognostic signature

Firstly, 515 patients were randomly assigned to a training dataset (n=258) and a testing dataset (n=257). The baseline characteristics of these patients are summarized in *Table 1*.

The training cohort was employed to construct the risk prognostic signature, which was validated with the testing cohort. Univariate analysis was performed to identify the cuproptosis-related lncRNAs notably associated with survival outcome in the training cohort using the R package "survival" ($P<0.01$). Subsequently, least absolute shrinkage and selection operator (LASSO) regression analysis with the 10-fold cross-check was used to remove the prognosis-related lncRNAs obviously related to each other to avoid overfitting using the R package "glmnet". Finally, 7 cuproptosis-related lncRNAs significantly related to prognosis were identified to establish a risk signature based on the RNA expression and coefficient. The risk score of each sample was calculated by the following format:

$$RiskScore = \sum_{i=1}^{n} Expi \times \beta i \quad [1]$$

In which n, Expi, and βi respectively refer to the number of lncRNAs in the signature, lncRNA expression level, and regression coefficient of each lncRNA.

Then, the samples were assigned to a low-risk group and a high-risk group with the cut-off value being median risk score. Kaplan–Meier curves were drawn to evaluate the survival outcomes of the 2 risk groups using the R package "survival". Additionally, a receiver operating characteristic (ROC) curve was drawn to estimate the 1-, 3-, and 5-year OS of KIRC patients using the R package "ROC".

Construction of a prognostic nomogram

Univariate analysis was conducted to evaluate the predictive ability of age, gender, grade, and AJCC stage for risk score and other clinicopathological features. Multivariate analysis was used to identify the independent prognostic role of them. Then, a nomogram was constructed with risk score and traditional clinical features related to prognosis via the stepwise regression model to estimate the 1-, 3-, and 5-year OS of KIRC patients. Afterward, calibration curves and the concordance index were performed to estimate the accuracy and reliability of the nomogram. Additionally, ROC curves were drawn and the areas under the curve (AUCs) were applied to assess the accuracy of the risk signature compared to other clinicopathological features, AUC >0.7 was considered to be effective.

Functional enrichment analysis

To further explore the underlying biological processes and cellular pathways of this prognosis relevance, Gene Ontology (GO) and Kyoto Encyclopedia of Genes and Genomes (KEGG) analyses were used in the R package "clusterProfiler" based on the differentially expressed genes (DEGs) between the 2 risk groups with $|\log2FC| \geq 1$, FDR <0.05.

Evaluation of tumor immune dysfunction and exclusion (TIDE) between the two risk groups

The tumor immune dysfunction and exclusion (TIDE) algorithm was performed to evaluate the response to ICIs response in KIRC. TIDE is the computational approach to model 2 major mechanisms in tumor immune evasion, including the induction of T cell dysfunction with high cytotoxic T lymphocyte (CTL) infiltration and the prevention of T cell infiltration with low CTL levels (12).

Potential new target drug candidates for KIRC

We explored the response to small molecule inhibitors for KIRC patients of the 2 risk groups based on the Genomics of Drug Sensitivity in Cancer (GDSC) database. We utilized the half maximal inhibitory concentration (IC_{50}) calculated by R package "pRRophetic" to assess the response to small molecule inhibitors, and obtained the potential new target candidates for KIRC patients.

Table 1 Clinical characteristics of KIRC patients in training and testing datasets

Covariates	Type	Total, n (%)	Group, n (%)		P value
			Testing	Training	
Age (years)					0.8041
	≤65	341 (66.21)	172 (66.93)	169 (65.5)	
	>65	174 (33.79)	85 (33.07)	89 (34.5)	
Gender					0.8279
	Female	177 (34.37)	90 (35.02)	87 (33.72)	
	Male	338 (65.63)	167 (64.98)	171 (66.28)	
Grade					0.5697
	G1	12 (2.33)	8 (3.11)	4 (1.55)	
	G2	220 (42.72)	112 (43.58)	108 (41.86)	
	G3	201 (39.03)	95 (36.96)	106 (41.09)	
	G4	74 (14.37)	36 (14.01)	38 (14.73)	
	Unknown	8 (1.55)	6 (2.33)	2 (0.78)	
Tumor stage					0.5534
	I	256 (49.71)	134 (52.14)	122 (47.29)	
	II	56 (10.87)	27 (10.51)	29 (11.24)	
	III	117 (22.72)	58 (22.57)	59 (22.87)	
	IV	83 (16.12)	36 (14.01)	47 (18.22)	
	Unknown	3 (0.58)	2 (0.78)	1 (0.39)	
Stage					
T					0.6907
	T1	262 (50.87)	136 (52.92)	126 (48.84)	
	T2	68 (13.2)	33 (12.84)	35 (13.57)	
	T3	174 (33.79)	84 (32.68)	90 (34.88)	
	T4	11 (2.14)	4 (1.56)	7 (2.71)	
M					0.5236
	M0	408 (79.22)	205 (79.77)	203 (78.68)	
	M1	79 (15.34)	36 (14.01)	43 (16.67)	
	Unknown	28 (5.44)	16 (6.23)	12 (4.65)	
N					0.2465
	N0	230 (44.66)	114 (44.36)	116 (44.96)	
	N1	16 (3.11)	5 (1.95)	11 (4.26)	
	Unknown	269 (52.23)	138 (53.7)	131 (50.78)	

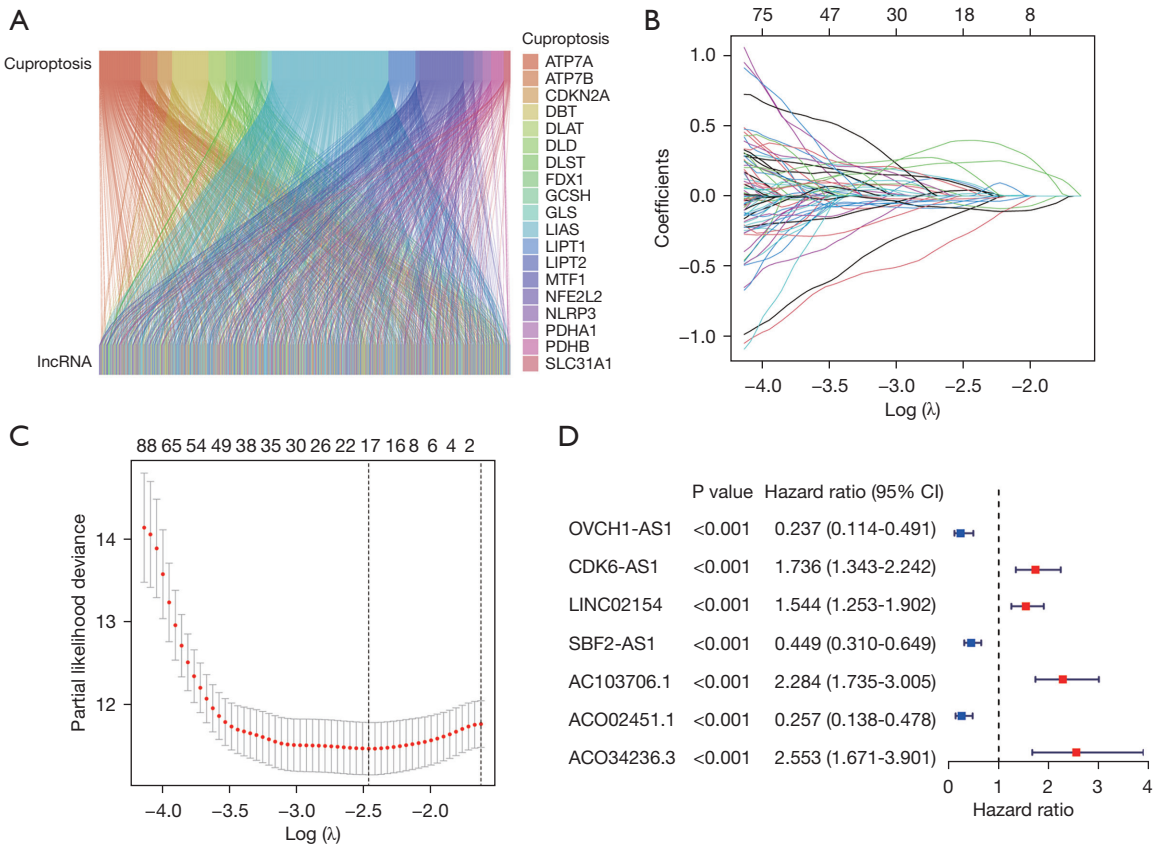

Figure 2 Construction of the cuproptosis-related lncRNAs signature. (A) Correlation analysis between 19 cuproptosis-related genes and 16,876 lncRNAs. (B) LASSO regression analysis. (C) Selection of the optimal penalty parameter for LASSO regression. (D) Univariate Cox regression analysis. LASSO, least absolute shrinkage and selection operator; lncRNA, long non-coding RNA.

Statistical analysis

We performed all the statistical analysis in R software (version 4.0.2; The R Foundation for Statistical Computing, Vienna, Austria). Kaplan-Meier analysis was used to evaluate the survival status. Univariate, LASSO, and multivariate analyses were performed to assess the prognostic value. The AUC was applied to assess the accuracy of the risk signature. A two-sided P value <0.05 indicated statistical significance.

Results

Construction of a cuproptosis-related lncRNA prognostic signature

Univariate Cox regression analysis was used to identify the cuproptosis-related lncRNAs significantly associated with the outcome of the patients with KIRC in the training cohort (*Figure 2A*). Subsequently, LASSO Cox regression analysis was used to eliminate the candidate lncRNAs, and the included lncRNAs were further evaluated through multivariate analysis (*Figure 2B*). Finally, 7 cuproptosis-related lncRNAs with predictive value were identified to construct the prognostic risk signature with the normalized expression level of the genes and their regression coefficients. Among them, OVCH1-AS1, SBF2-AS1, and AC002451.1 were protective factors with hazard ratio (HR) <1, whereas CDK6-AS1, LINC02154, AC103706.1, and AC034236.3 were pernicious factors with HR >1 (*Figure 2C,2D*). Moreover, Kaplan-Meier analysis was performed to assess the prognostic role of these 7 lncRNAs, and revealed that lower expression of OVCH1-AS1, SBF2-AS1, and AC002451.1 and higher expression levels of CDK6-AS1, LINC02154, AC103706.1, and AC034236.3 were related to a less favorable survival outcome (Figure S1).

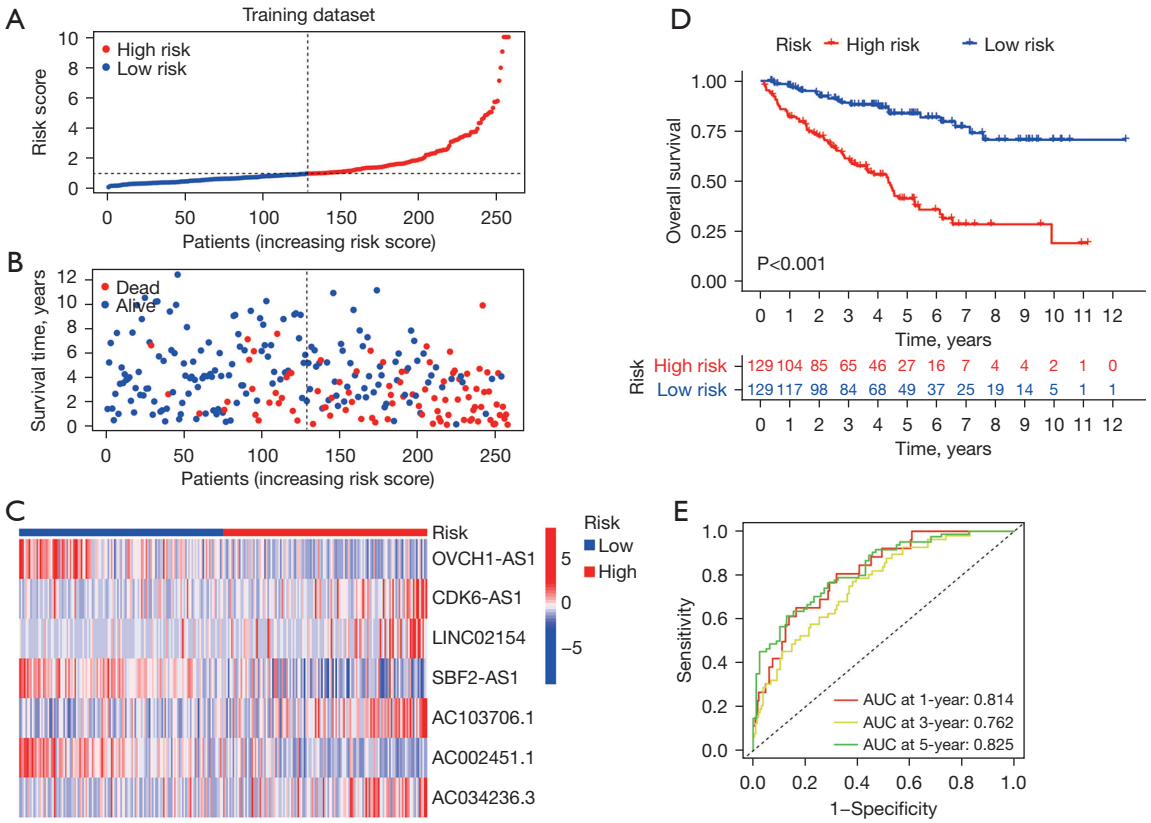

Figure 3 Validation of the cuproptosis-related lncRNA prognostic signature in the training group. (A) Risk score rank. (B) Survival status map. (C) Expression heatmap of 7 signature lncRNAs. (D) Survival curve. (E) ROC curve. lncRNA, long non-coding RNA; ROC, receiver operating characteristic.

Validation of the cuproptosis-related lncRNA prognostic signature

To evaluate the reliability and sensitivity of the prognostic risk-related signature, the risk scores were calculated by the formula in the method and the patients were assigned to either the low-risk group or the high-risk group based on the median risk score in the training cohort. The scatter plot indicated that the high-risk cohort was more closely related to a high mortality rate than the low-risk cohort, the survival rates were 44.96% and 83.72%, respectively (P<0.001) (*Figure 3A*,*3B*). In addition, the heatmap showed that the detrimental factors CDK6-AS1, LINC02154, AC103706.1, and AC034236.3 were all highly expressed in the high-risk cohort (*Figure 3C*). The Kaplan-Meier survival curves revealed that the KIRC patients in the high-risk cohort had less favorable survival outcomes than those in the low-risk cohort (*Figure 3D*). In addition, the AUC value for 1, 3, 5-year survival rate reached 0.814, 0.762 and 0.825, respectively (*Figure 3E*), which suggested that the signature had a high predictive capacity in the training dataset.

To further verify the predictive ability of the risk signature, we applied the same algorithm to compute the risk score in the testing and overall datasets (*Figure 4*). The results were similar to those in the training dataset. For the testing dataset, the survival rates of high- and low-risk cohorts were 54.70% and 81.43% (P<0.001). And, the AUC value for 1-, 3-, 5-year survival rate was 0.724, 0.746, and 0.743, respectively. Similarly, for the entire dataset, the survival rates of high- and low-risk cohorts were 49.59% and 82.53% (P<0.001). And, the AUC value for 1-, 3-, 5-year survival rate was 0.772, 0.753, and 0.785, respectively. The above results suggested that the high-risk score indicates an unfavorable prognosis, accurately.

Construction and evaluation of a predictive nomogram

To evaluate the prognostic value of the cuproptosis-

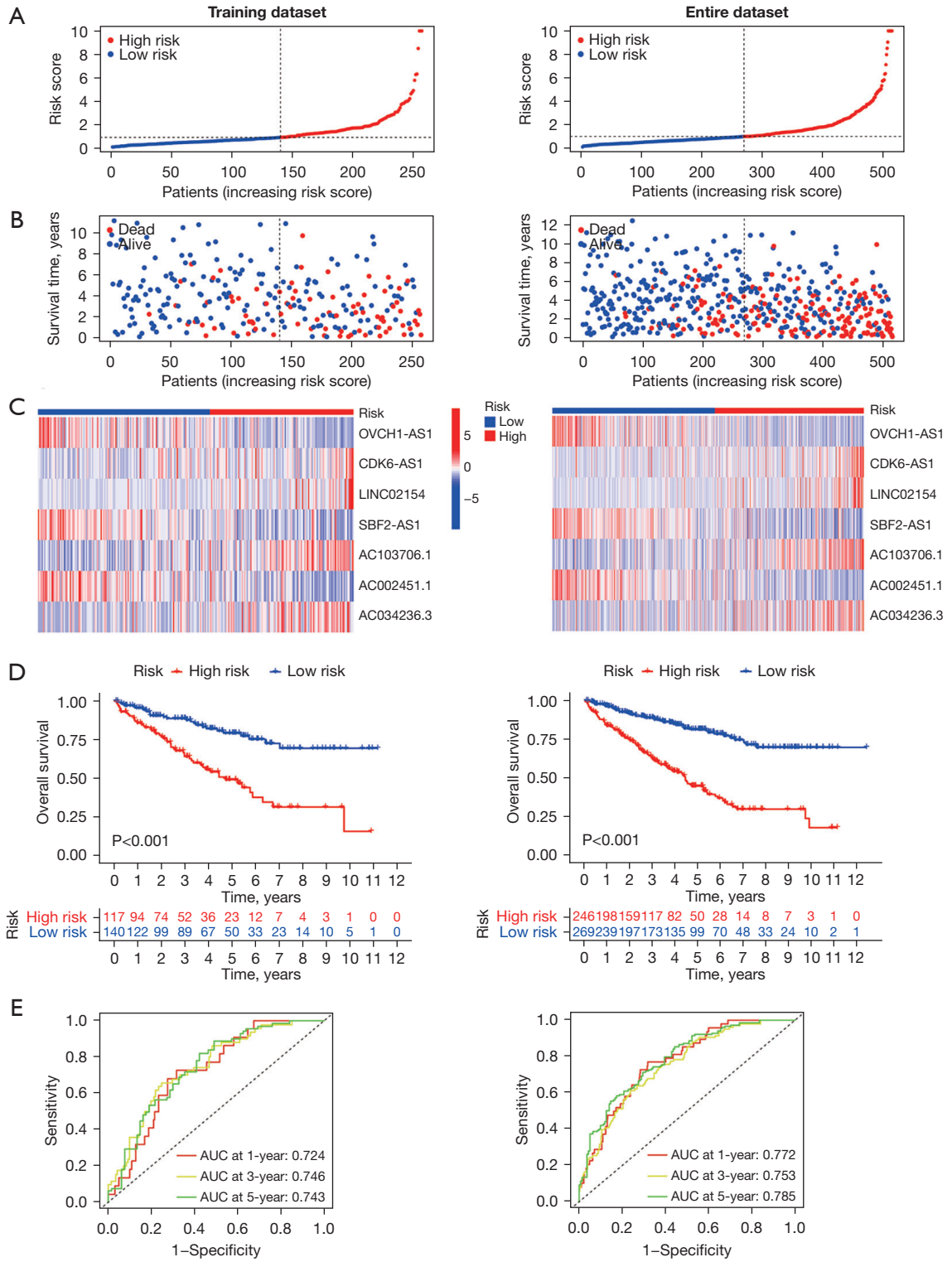

Figure 4 Validation of the cuproptosis-related lncRNA prognostic signature in the testing and entire group. (A) Risk score rank. (B) Survival status map. (C) Expression heatmap of 7 signature lncRNAs. (D) Survival curve. (E) ROC curve. lncRNA, long non-coding RNA; ROC, receiver operating characteristic.

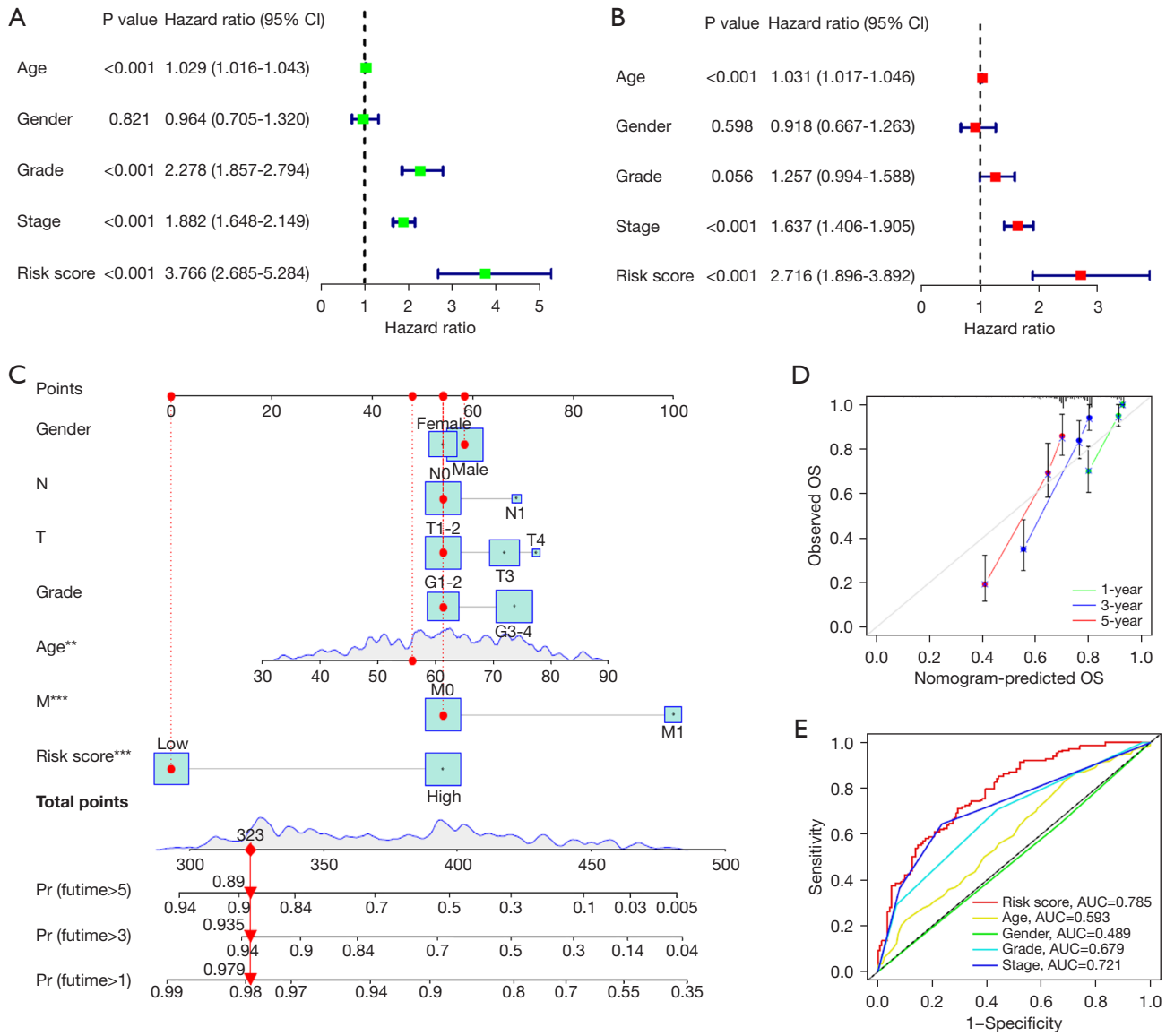

Figure 5 Construction and evaluation of a predictive nomogram. (A) Univariate Cox regression analysis. (B) Multivariate Cox regression analysis. (C) A nomogram model to predict the 1-, 3-, and 5-year OS. (D) Calibration curves of the nomogram to predict the 1-, 3-, and 5-year OS. (E) The AUC values for risk score and other clinicopathological parameters. **P<0.01, ***P<0.001. OS, overall survival; AUC, area under the curve; Pr, probability.

related signature, univariate and multivariate analyses were performed. The results demonstrated that grade, stage, and risk score were prognostic indicators in KIRC (*Figure 5A*). After adjusting for other prognostic factors (age, grade, and stage), the signature remained a significant independent prognostic factor (*Figure 5B*). Moreover, we used a quantitative method with the risk score and traditional clinical variables to construct a nomogram (*Figure 5C*). The calibration plot for 1-, 3-, and 5-year survival probability indicated an optimal consistency between predictive and observation curves (*Figure 5D*). In addition, multivariate ROC curves of the risk score and clinical variables showed that the AUC value for risk score was 0.785 higher than that for age (0.593), gender (0.489), grade (0.679), and stage (0.721) (*Figure 5E*). Taken together, the results indicated that the signature has promising clinical applicability.

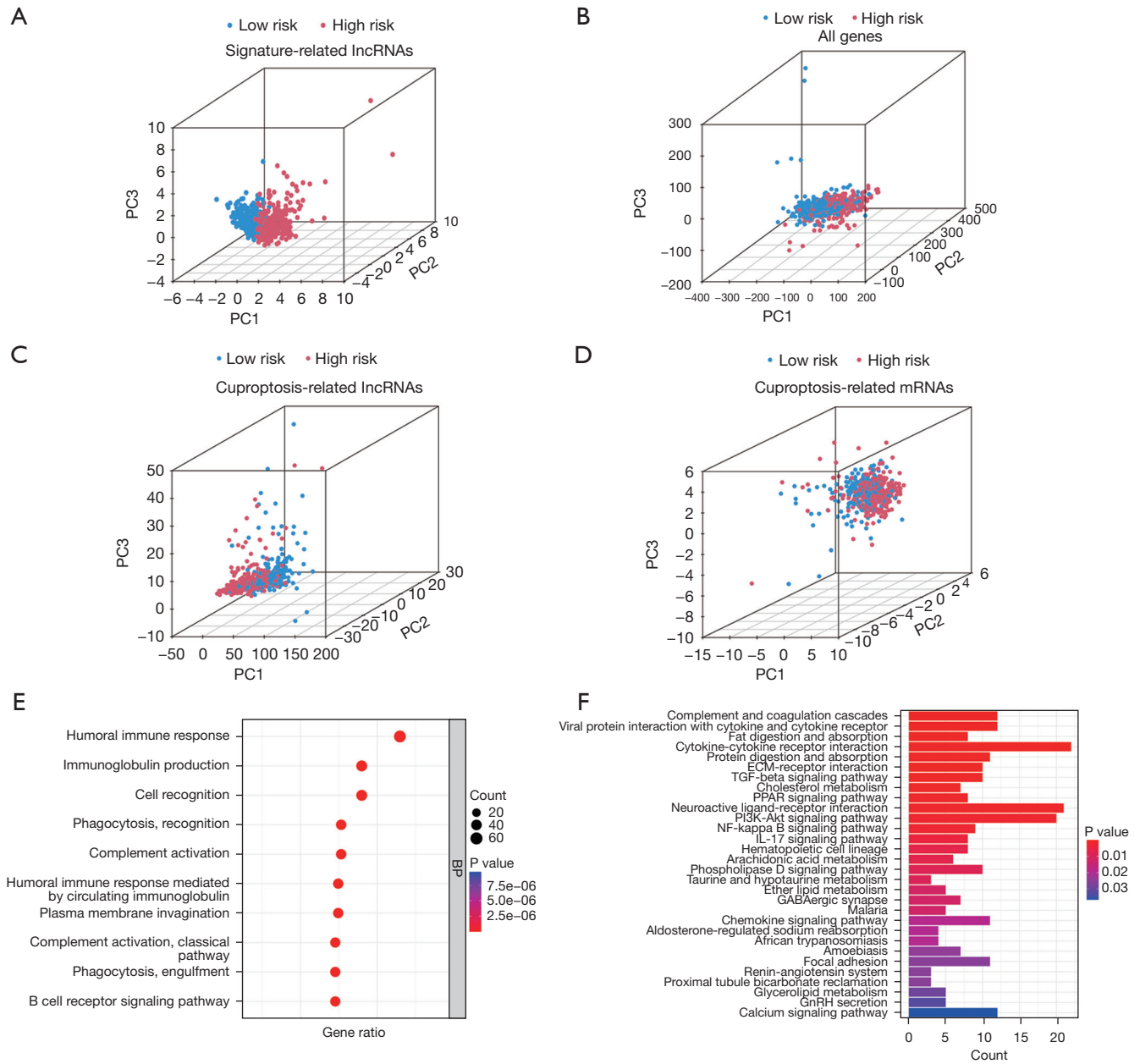

Figure 6 Function Enrichment Analysis. (A-D) PCA based on signature-related lncRNAs, all genes, cuproptosis-related lncRNAs, and cuproptosis-related mRNAs. (E) Top 10 of GO-BP enrichment. (F) Top 30 of KEGG pathways. BP, biological process; PCA, principal component analysis; lncRNA, long non-coding RNA; KEGG, Kyoto Encyclopedia of Genes and Genomes; GO, Gene Ontology.

Functional enrichment analyses based on the risk signature

Principal component analysis (PCA) was used to explore the heterogeneity between the 2 risk cohorts to validate the stratification ability of the signature based on signature-related lncRNAs, all genes, cuproptosis-related lncRNAs, and cuproptosis-related mRNAs. As shown in *Figure 6A-6D*, the 2 risk cohorts showed diverse distribution directions based on our signature, which validated the efficacy of our prognostic signature distinguishing low- and high-risk populations.

Next, GO enrichment and KEGG pathway analyses were used according to the DEGs between the 2 risk groups

to further explore the potential biological mechanisms and pathways that are related to the signature. The results of GO analysis showed that phagocytosis, humoral immune response, complement activation, and B cell receptor signaling pathway were mainly enriched (*Figure 6E*). Likewise, KEGG analyses found that genes were mainly enriched in the cytokine-cytokine receptor interaction, transforming growth factor-beta (TGF-β), interleukin-17 (IL-17) signaling pathway, and nuclear factor (NF)-kappa B (*Figure 6F*). These results indicated that the DEGs were significantly enriched in the immune-related signaling pathway.

Immune status differential analysis between the two risk groups

To further understand the immune function of these 7 cuproptosis-related lncRNAs, the single sample gene set enrichment analysis (ssGSEA) analyzed the differences in 13 types of immune signal pathways between the 2 risk groups. The high-risk group exhibited activation in the immune pathways, including the APC co-inhibition and co-stimulation, immune checkpoints, cytolytic activity, and T cell co-inhibition and co-stimulation (*Figure 7A*). Considering the clinical application and benefits of ICIs, we next analyzed 22 kinds of the immune cell infiltrations and 38 immune checkpoints. The results revealed that the high-risk group had increased infiltrations of the activated B cell, activated dendritic cell, activated T cell, macrophage, MDSC cell, monocyte, and NK T cell, and decreased infiltrations of the immature dendritic cell and neutrophil compared to the low-risk group (*Figure 7B*). Besides, most immune checkpoints, such as *BTLA*, *CD27*, *CD28*, *CD40LG*, *CD44*, *CD48*, *CD70*, *CD80*, *CD86*, *CD244*, *CD2000R1*, *CTLA4*, *IDO2*, *ICOS*, *LAIR1*, *LAG3*, *LGALS9*, *PDCD1(PD-1)*, *TMIGD2*, *TNFRSF9*, *TNFRSF25*, *TNFRSF8*, *TIGIT*, *TNFSF14*, *TNFRSF18*, were positively associated with the risk scores (*Figure 7C*). We were curious about which factors mediated by the signature lncRNAs play a dominant role in the immune function of KIRC: immunosuppressive or immune activating factors. Therefore, we further scored the TIDE, and the results showed that the high-risk group indicated a higher TIDE score (*Figure 7D*), which means that the high-risk group had a stronger immune escape ability. Overall, the patients in low-risk group tended to benefit from immunotherapy.

Drug sensitivity differential analysis between the two risk groups

In addition to immunotherapy, we also explored the correlation of the risk signature with the efficacy of small molecule inhibitors for KIRC. These results showed that the IC_{50} of pyrimethamine, MS-275, and CGP-60474 in the high-risk group was lower, and that of GSK1904529A, tipifarnib, BX-912, FR-180204, and GSK1070916 was higher in the high-risk group (*Figure 8*), which contributed to explore the individualized agents suitable for subgroup of KIRC patients.

Discussion

As the primary subtype of RCC, KIRC is characterized by high metastatic potential, heterogeneity, and immune-responsive tumors (13). Although the incidence of KIRC is increasing, the survival of advanced RCC patients has been significantly improved with molecularly targeted drug combinations and ICIs (14,15). However, the complexity of the TME in RCC leads to drug resistance, insufficient therapeutic response, and relapse during treatment (16,17). Therefore, it is of vital importance to construct more accurate prognostic models to estimate the prognosis and therapeutic response of novel treatment targets in KIRC.

Cuproptosis is an unconventional mechanism of RCD and may provide novel insights in exploiting Cu toxicity to treat cancers (18). In addition, there are some new findings on the pathology of the urinary tract. Cu has been found to contribute to reducing the bacterial colonization in the urethra, which may provide directions for potential treatments.

This study is the first to explore the clinical value of cuproptosis-related lncRNAs in KIRC. In our study, we carried out a comprehensive analysis of cuproptosis-related lncRNAs in KIRC and identified 7 prognosis-related lncRNAs (OVCH1-AS1, SBF2-AS1, AC002451.1, CDK6-AS1, LINC02154, AC103706.1, and AC034236.3) to construct a risk signature which could accurately estimate the prognosis of KIRC patients (*Figures 1-4*).

Of the 7 signature lncRNAs, CDK6-AS1, LINC02154, AC103706.1, and AC034236.3 were upregulated and were correlated with poor survival. In contrast, OVCH1-AS1, SBF2-AS1, and AC002451.1 were downregulated and acted as protective factors (Figures S1,S2). Among

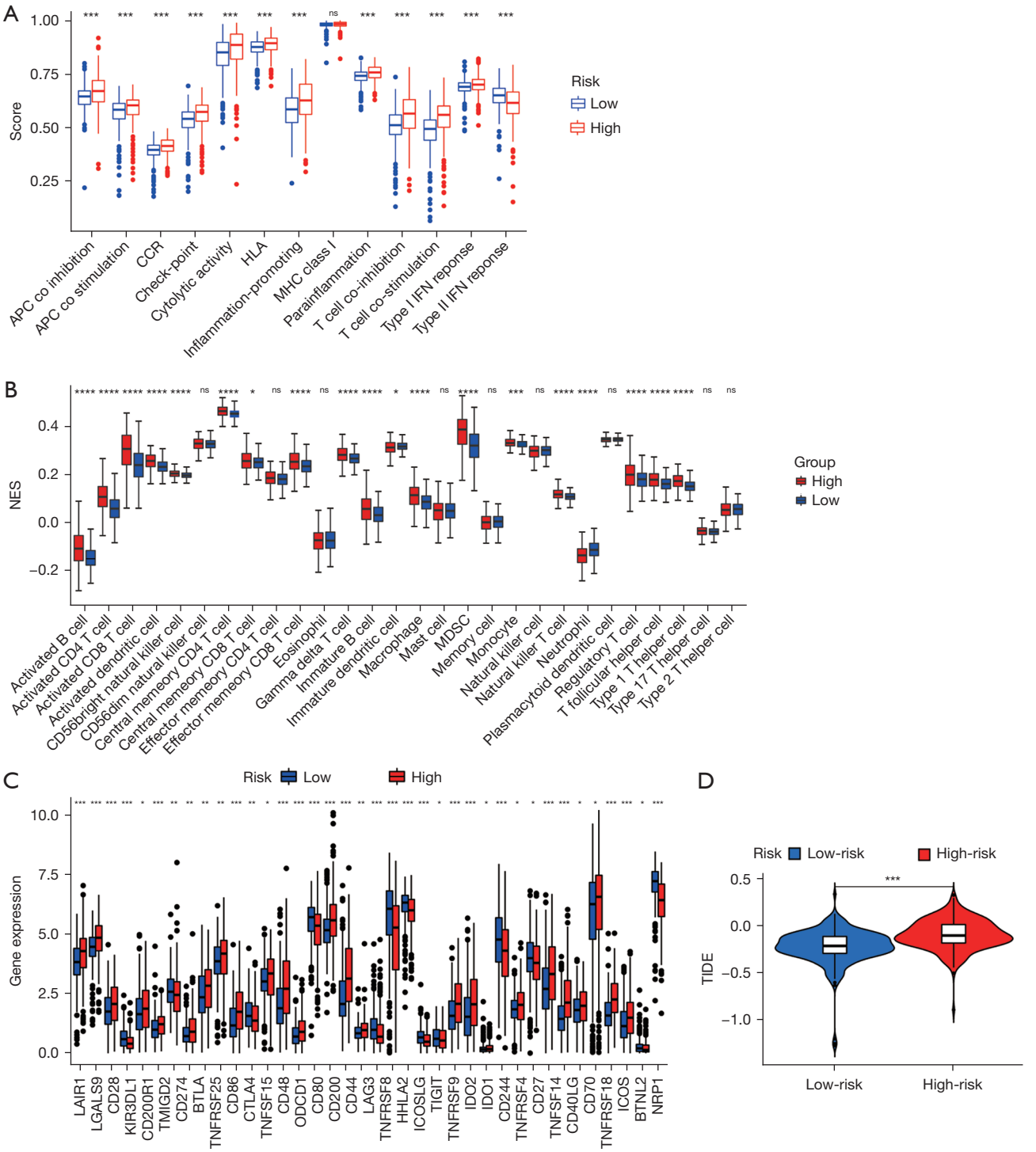

Figure 7 Immune status analysis. (A) Immune function differential analysis. (B) Immune cell infiltration differential analysis. (C) Immune checkpoints differential analysis. (D) TIDE score. *P<0.05, **P<0.01, ***P<0.001, ****P<0.0001, ns, no significance. NES, normalized enrichment score; TIDE, tumor immune dysfunction and exclusion.

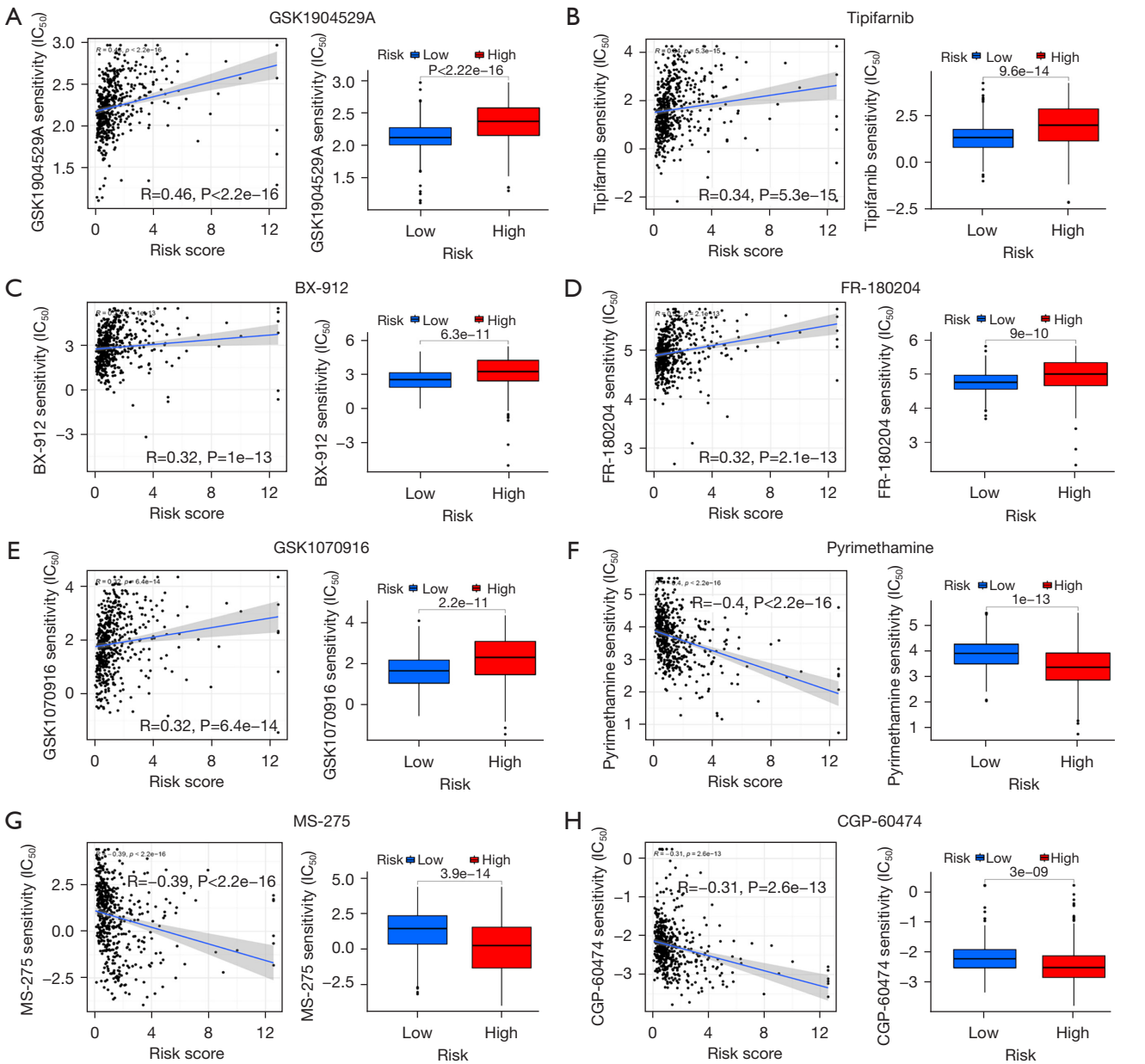

Figure 8 Drug sensitivity analysis. (A) GSK1904529A. (B) Tipifarnib. (C) BX-912. (D) FR-180204. (E) GSK1070916. (F) Pyrimethamine. (G) MS-275. (H) CGP-60474.

them, OVCH1 (ovochymase) encodes oocyte extracellular polyproteins (19), which has been reported in familial Meniere's disease (20) and early-onset myasthenia gravis (21), but its function in other cells has not yet been described. OVCH1-AS1 is transcribed from the antisense strand of the *OVCH1* gene, which may act the opposite effect. We observed an increased expression of OVCH1-AS1 in the high-risk group of KIRC patients. SET binding factor 2-antisense strand 1 (SBF2-AS1) encodes myotubularin-related protein 13 (MTMR13) (22). SBF2-AS1 is a newly discovered lncRNA, which has been confirmed to be highly expressed in various cancers and involved in promoting tumorigenesis, progression, and metastasis. Furthermore, SBF2-AS1 upregulation was significantly associated with unfavorable clinicopathological features, suggesting a poor prognosis (23). CDK6-AS1 is a lncRNA cyclin-

dependent kinase 6 and regulates cell migration and invasion in a synergic manner with CDK6 (24), which may act as a potential prognostic candidate biomarker in gastric cancer (25). AC002451 is one of the ferroptosis-related lncRNAs related to poor prognosis of gastric adenocarcinoma (26). Some studies have shown that linc02154 may serve as a valuable biomarker to predict the prognosis and indicate the immune status in laryngeal squamous cell carcinoma and as a potential therapeutic target (27-29). Another study indicated that LINC02154 facilitates hepatocellular carcinoma proliferation and metastasis by enhancing SPC24 promoter activity and activating the PI3K-AKT signaling pathway (30). However, the other 2 genes, AC103706.1 and AC034236.3, have not been previously reported. This study first found that they could serve as the potential prognostic biomarkers of KIRC.

In view of the immune-related signaling pathways were significantly enriched in GO and KEGG analyses (*Figure 6*), we subsequently evaluated the immune-related functions based on the score comparisons. We found that the high-risk group had higher scores in many immune signal pathways (the APC co-inhibition and co-stimulation, immune checkpoints, cytolytic activity, and T cell co-inhibition and co-stimulation, *Figure 7A*), immune cell infiltration (activated T cell, activated dendritic cell, activated B cell, macrophage, MDSC cell, monocyte, and NK T cell, *Figure 7B*), and immune checkpoints (BTLA, CD27, CD28, CD44, CD48, CD70, CD80, CD86, CD244, CTLA4, IDO2, ICOS, LAIR1, LAG3, and PD-1, etc., *Figure 7C*), which may critically affect the immunotherapeutic efficacy and resistance.

Studies have revealed that various factors, such as programmed death ligand-1 (PD-L1) level (31), the degree of cytotoxic T cell infiltration (32), antigen presentation defects (33), mutation (34), and interferon signaling (35), can affect the effectiveness of ICIs (36). However, none of them these factors are sufficient to achieve accurate prognostic prediction (37). A recent study showed 2 distinct tumor immune evasion mechanisms. The cytotoxic T cells with high infiltration level tend to be in a dysfunctional state in some tumors. And in other tumors, the immunosuppressive factors may prevent the T cells from infiltrating tumors (38). Thus, Jiang *et al.* developed TIDE to identify the factors underlying these 2 immune escape mechanisms (12). Compared with the widely used response biomarkers of ICIs, PD-L1 level and tumor mutation burden (TMB) (37,39), the TIDE achieved the same favorable and robust prediction capacity for both anti-CTLA4 and anti-PD1 therapies. Several recent studies have reported its utility in predicting or evaluating the therapeutic efficacy of ICIs (12,40). Therefore, we used TIDE to predict the response of ICIs. The analysis results revealed that the risk signature had promising potential to indicate the response to immunotherapy in KIRC patients, and that the patients with low-risk scores tended to benefit from the immunotherapy (*Figure 7D*).

Drug resistance is still a challenge for clinical management of tumor patients. Many patients may face the dilemma of no drug availability after multi-line anti-tumor therapy. The development of new drugs is a tortuous, expensive, and highly uncertain process. Computational drug repurposing or repositioning is an efficient and promising tool to discover new applications from the existing drugs (41). We evaluated the sensitivities of multiple antitumor drugs, and the results indicated that the patients with low-risk scores were more sensitive to the small molecular drugs GSK1904529A (an insulin-like growth factor-1 receptor and insulin receptor inhibitor), tipifarnib (a farnesyltransferase inhibitor), BX-912 (a PDK1 inhibitor), FR-180204 (an ERK inhibitor), and GSK1070916 (an aurora B and aurora C inhibitor). Meanwhile, the high-risk group tended to be more sensitive to pyrimethamine, MS-275 (a HDAC class I inhibitor), and CGP-60474 (a CDK inhibitor) (*Figure 8*). These results provided candidate drugs for preclinical and clinical treatment for KIRC patients in different subgroups.

Conclusions

In summary, we identified the important role of cuproptosis-related lncRNAs in KIRC and constructed a novel cuproptosis-related lncRNA signature, which might serve as a promising biomarker for predicting the prognosis of KIRC patients. However, there were several limitations to our study. First, our findings were mainly based on the integrated bioinformatical analysis and lacked experimental verification at the cellular level, including function verification and regulation mechanism research, which is still needed. Second, all of the datasets in our study were extracted from a public database, which may have led to a potential bias in clinical and genetic data. However, cross-validation was performed among independent datasets as much as possible to reduce potential bias. Third, our study needs further clinical verification to validate its application in clinic.

Acknowledgments

We are grateful to the contributors of the public databases used in this study.

Funding: This study was supported by the Henan Provincial Science and Technology Research Project (202102310157).

Footnote

Reporting Checklist: The authors have completed the TRIPOD reporting checklist. Available at https://atm.amegroups.com/article/view/10.21037/atm-22-5204/rc

Conflicts of Interest: All authors have completed the ICMJE uniform disclosure form (available at https://atm.amegroups.com/article/view/10.21037/atm-22-5204/coif). The authors have no conflicts of interest to declare.

Ethical Statement: The authors are accountable for all aspects of the work in ensuring that questions related to the accuracy or integrity of any part of the work are appropriately investigated and resolved. The study was conducted in accordance with the Declaration of Helsinki (as revised in 2013).

References

1. Escudier B, Porta C, Schmidinger M, et al. Renal cell carcinoma: ESMO Clinical Practice Guidelines for diagnosis, treatment and follow-up†. Ann Oncol 2019;30:706-20.
2. Díaz-Montero CM, Rini BI, Finke JH. The immunology of renal cell carcinoma. Nat Rev Nephrol 2020;16:721-35.
3. Jonasch E, Walker CL, Rathmell WK. Clear cell renal cell carcinoma ontogeny and mechanisms of lethality. Nat Rev Nephrol 2021;17:245-61.
4. Barata PC, Rini BI. Treatment of renal cell carcinoma: Current status and future directions. CA Cancer J Clin 2017;67:507-24.
5. Wolf MM, Kimryn Rathmell W, Beckermann KE. Modeling clear cell renal cell carcinoma and therapeutic implications. Oncogene 2020;39:3413-26.
6. Makhov P, Joshi S, Ghatalia P, et al. Resistance to Systemic Therapies in Clear Cell Renal Cell Carcinoma: Mechanisms and Management Strategies. Mol Cancer Ther 2018;17:1355-64.
7. Kotecha RR, Motzer RJ, Voss MH. Towards individualized therapy for metastatic renal cell carcinoma. Nat Rev Clin Oncol 2019;16:621-33.
8. Jiang Y, Huo Z, Qi X, et al. Copper-induced tumor cell death mechanisms and antitumor theragnostic applications of copper complexes. Nanomedicine (Lond) 2022;17:303-24.
9. Shanbhag VC, Gudekar N, Jasmer K, et al. Copper metabolism as a unique vulnerability in cancer. Biochim Biophys Acta Mol Cell Res 2021;1868:118893.
10. Li D, Liang J, Cheng C, et al. Identification of m6A-Related lncRNAs Associated With Prognoses and Immune Responses in Acute Myeloid Leukemia. Front Cell Dev Biol 2021;9:770451.
11. Yu J, Mao W, Sun S, et al. Identification of an m6A-Related lncRNA Signature for Predicting the Prognosis in Patients With Kidney Renal Clear Cell Carcinoma. Front Oncol 2021;11:663263.
12. Jiang P, Gu S, Pan D, et al. Signatures of T cell dysfunction and exclusion predict cancer immunotherapy response. Nat Med 2018;24:1550-8.
13. Znaor A, Lortet-Tieulent J, Laversanne M, et al. International variations and trends in renal cell carcinoma incidence and mortality. Eur Urol 2015;67:519-30.
14. Pal SK, McGregor B, Suárez C, et al. Cabozantinib in Combination With Atezolizumab for Advanced Renal Cell Carcinoma: Results From the COSMIC-021 Study. J Clin Oncol 2021;39:3725-36.
15. Bedke J, Albiges L, Capitanio U, et al. The 2021 Updated European Association of Urology Guidelines on Renal Cell Carcinoma: Immune Checkpoint Inhibitor-based Combination Therapies for Treatment-naive Metastatic Clear-cell Renal Cell Carcinoma Are Standard of Care. Eur Urol 2021;80:393-7.
16. Au L, Hatipoglu E, Robert de Massy M, et al. Determinants of anti-PD-1 response and resistance in clear cell renal cell carcinoma. Cancer Cell 2021;39:1497-1518.e11.
17. Di Bona C, Stühler V, Rausch S, et al. Pembrolizumab for the treatment of renal cell carcinoma. Expert Opin Biol

Ther 2021;21:1157-64.
18. Wang Y, Zhang L, Zhou F. Cuproptosis: a new form of programmed cell death. Cell Mol Immunol 2022;19:867-8.
19. Mino M, Sawada H. Follicle cell trypsin-like protease HrOvochymase: Its cDNA cloning, localization, and involvement in the late stage of oogenesis in the ascidian Halocynthia roretzi. Mol Reprod Dev 2016;83:347-58.
20. Skarp S, Korvala J, Kotimaki J, et al. New Genetic Variants in CYP2B6 and SLC6A Support the Role of Oxidative Stress in Familial Meniere's Disease. Genes (Basel) 2022;13:998.
21. Varade J, Wang N, Lim CK, et al. Novel genetic loci associated HLA-B*08:01 positive myasthenia gravis. J Autoimmun 2018;88:43-9.
22. Lv J, Qiu M, Xia W, et al. High expression of long non-coding RNA SBF2-AS1 promotes proliferation in non-small cell lung cancer. J Exp Clin Cancer Res 2016;35:75.
23. Lu Q, Lou J, Cai R, et al. Emerging roles of a pivotal lncRNA SBF2-AS1 in cancers. Cancer Cell Int 2021;21:417.
24. Liu J, Wang Y, Chen P, et al. AC002454.1 and CDK6 synergistically promote endometrial cell migration and invasion in endometriosis. Reproduction 2019;157:535-43.
25. Yang S, Zou X, Yang H, et al. Identification of Enhancer RNA CDK6-AS1 as a Potential Novel Prognostic Biomarker in Gastric Cancer. Front Genet 2022;13:854211.
26. Cai Y, Wu S, Jia Y, et al. Potential Key Markers for Predicting the Prognosis of Gastric Adenocarcinoma Based on the Expression of Ferroptosis-Related lncRNA. J Immunol Res 2022;2022:1249290.
27. Zhang G, Fan E, Zhong Q, et al. Identification and potential mechanisms of a 4-lncRNA signature that predicts prognosis in patients with laryngeal cancer. Hum Genomics 2019;13:36.
28. Qian L, Ni T, Fei B, et al. An immune-related lncRNA pairs signature to identify the prognosis and predict the immune landscape of laryngeal squamous cell carcinoma. BMC Cancer 2022;22:545.
29. Gong S, Xu M, Zhang Y, et al. The Prognostic Signature and Potential Target Genes of Six Long Non-coding RNA in Laryngeal Squamous Cell Carcinoma. Front Genet 2020;11:413.
30. Yue H, Wu K, Liu K, et al. LINC02154 promotes the proliferation and metastasis of hepatocellular carcinoma by enhancing SPC24 promoter activity and activating the PI3K-AKT signaling pathway. Cell Oncol (Dordr) 2022;45:447-62.
31. Cha JH, Chan LC, Li CW, et al. Mechanisms Controlling PD-L1 Expression in Cancer. Mol Cell 2019;76:359-70.
32. Wang H, Kaur G, Sankin AI, et al. Immune checkpoint blockade and CAR-T cell therapy in hematologic malignancies. J Hematol Oncol 2019;12:59.
33. Gu SS, Zhang W, Wang X, et al. Therapeutically Increasing MHC-I Expression Potentiates Immune Checkpoint Blockade. Cancer Discov 2021;11:1524-41.
34. McGrail DJ, Pilié PG, Rashid NU, et al. High tumor mutation burden fails to predict immune checkpoint blockade response across all cancer types. Ann Oncol 2021;32:661-72.
35. Lam KC, Araya RE, Huang A, et al. Microbiota triggers STING-type I IFN-dependent monocyte reprogramming of the tumor microenvironment. Cell 2021;184:5338-5356.e21.
36. Morad G, Helmink BA, Sharma P, et al. Hallmarks of response, resistance, and toxicity to immune checkpoint blockade. Cell 2021;184:5309-37.
37. Nishino M, Ramaiya NH, Hatabu H, et al. Monitoring immune-checkpoint blockade: response evaluation and biomarker development. Nat Rev Clin Oncol 2017;14:655-68.
38. Spranger S, Gajewski TF. Tumor-intrinsic oncogene pathways mediating immune avoidance. Oncoimmunology 2016;5:e1086862.
39. Ayers M, Lunceford J, Nebozhyn M, et al. IFN-γ-related mRNA profile predicts clinical response to PD-1 blockade. J Clin Invest 2017;127:2930-40.
40. Ning XH, Li NY, Qi YY, et al. Identification of a Hypoxia-Related Gene Model for Predicting the Prognosis and Formulating the Treatment Strategies in Kidney Renal Clear Cell Carcinoma. Front Oncol 2021;11:806264.
41. Li J, Zheng S, Chen B, et al. A survey of current trends in computational drug repositioning. Brief Bioinform 2016;17:2-12.

(English Language Editor: J. Jones)

Cite this article as: Li D, Wu X, Song W, Cheng C, Hao L, Zhang W. Clinical significance and immune landscape of cuproptosis-related lncRNAs in kidney renal clear cell carcinoma: a bioinformatical analysis. Ann Transl Med 2022;10(22):1235. doi: 10.21037/atm-22-5204

